SIMULATION ON THERMO-PHYSICAL PROPERTIES OF FINE WOVEN PIERCED C/C COMPOSITE

LIANG Heng, TONG Mingbo, WANG Yuqing
Ministerial Key Discipline Laboratory of Advanced Design Technology of Aircraft, Nanjing University of Aeronautics and Astronautics, 29, Yudao Street, Nanjing, China
Email: tongw@nuaa.edu.cn

Keywords: Fine woven pierced C/C composites; unit cell; periodic boundary condition; thermo-physical properties

Abstract

Based on the meso and micro structures of fine woven pierced c/c composite, finite element models of single yarn and c/c composite are established respectively. By using the periodic boundary condition, the thermo-physical properties of composite are calculated. Furthermore, the law of thermo-physical properties by yarns volume fraction is studied. With the increasing of the yarn volume fraction, the transverse and longitudinal effective thermal conductivities decrease and the thermal expansion coefficient do not differ much, which provides a useful reference for the analysis of thermal and thermo-mechanical coupling.

1. Introduction

Woven fabric C/C composites are widely used as important components in aerospace engineering due to their high specific stiffness and strength as well as their excellent thermo-physical properties. The composites are expected to experience a range of mechanical and thermal environment when they are used in spacecrafts as main structures [1]. The research on the properties of the composites has been more and more significant. Many researches have been conducted on this subject both experimentally and numerically [2-5]. Fine woven pierced C/C composites, a special sort of woven composites, are made of XY-directional interlaced yarns and Z-directional yarns. The properties of fine woven pierced C/C composites will differ from that of woven fabric composites with the effect of Z-directional yarns. Because of their complicated architecture and anisotropic nature, it is difficult and time consuming to fully predict the mechanical and thermal characteristics of these materials form experiment. Therefore, it is necessary to conduct a series of finite element models to evaluate their mechanical and thermal behavior.

Prediction of composite effective properties based on the representative volume element (RVE) has been of interest for many years. Two scales models are usually conducted to study composites properties: meso- and macro-scale, which correspond to study properties of yarns and woven fabric composites, respectively. Bigaud et al. [6] provided a method to calculate the effective thermal conductivity tensor of textile-reinforced composite. Farooqi and Sheikh [7] calculated the effective thermal conductivity of ceramic-matrix composites with periodicity vectors for the boundary conditions. Schuster et al. [8] investigated thermal conductivity of woven fabric composites. Hongzhou Li et al. [9] used unit cells at multiple length scales to prediction the effective thermal conductivities of woven fabric composites and study the law of thermal conductivities influenced by material parameters.

Excerpt from ISBN 978-3-00-053387-7

This work focuses on calculating the effective thermal conductivities and Thermal expansion coefficient of fine woven pierced c/c composites. Two unit cells with periodic boundary conditions are built to evaluate the properties at multiple length scales. Besides, the law of thermo-physical properties by material parameters (i.e. fiber volume fraction, fiber and matrix thermo-physical properties) are studied.

2. Methodology

2.1. Periodic boundary conditions

In the finite element analysis of heterogeneous materials, the proper boundary conditions are very significant to calculate results accurately. Assuming that, the fibers in woven composites are uniform and distributed according to a certain rule, the meso structure is periodicity obviously, the macro structure can be treated as generated by the same meso structures in a certain period. In this paper，woven fabric C/C composites are consisted of numbers of plain woven layers in XY direction and pierced by carbon fiber bundles in Z direction. Material shows translational symmetry obviously, the smallest translational symmetry unit is selected as the representative volume element, as shown in Fig.1.

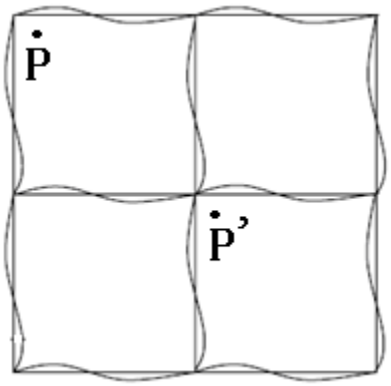

Figure 1 Figure of Unit Cell with translational symmetry

Based on the translational symmetry theory and assuming the unit cell is hexahedron as shown in Fig.2, any point P’(x’,y’,z’) in the unit cell can be found as the image of a certain point P(x,y,z) in a certain unit cell under a translational symmetry transformation consisting of up to three translation in the x, y and z directions. The relationships of these two points are as follows:

$$(x', y' z') = (x + ia, y + jb, z + kh) \tag{1}$$

where i, j, k =0, ±1, ±2,… are the numbers of cells by which P’(x’,y’,z’) is away from P(x,y,z) in the x, y and z directions, respectively.

Excerpt from ISBN 978-3-00-053387-7

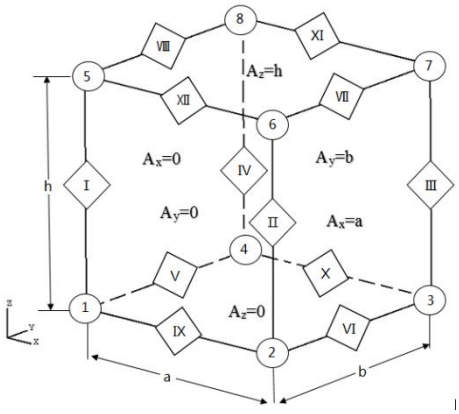

Figure 2 Unit Cell: cuboid and its faces, edges and vertices.

The relationship of temperature field between P'(x',y',z') and P(x,y,z) are as follows:

$$T'-T=\left(x'-x\right)T_x^0+\left(y'-y\right)T_y^0+\left(z'-z\right)T_z^0 \tag{2}$$

where T_x^0, T_y^0, T_z^0 are the macroscopic temperature gradients in the x, y and z directions, respectively.

Based on the translational symmetry theory, temperature field should also meet the translational symmetry conditions. Substituting the coordinate relations in Eq.(1) into Eq.(2), one obtains

$$T'-T=iaT_x^0+jbT_y^0+khT_z^0 \tag{3}$$

With translational symmetry transformations, the three faces of the hexahedron can be treated as the image of the faces in adjacent hexahedron with one translation transformation in *x*, *y* and *z* directions, respectively. Thus, the temperature boundary conditions on the three paired faces can be obtained in the form of equations as,

$$\begin{cases} T_{x=a}-T_{x=0}=aT_x^0 \\ T_{y=b}-T_{y=0}=bT_y^0 \\ T_{z=h}-T_{z=0}=hT_z^0 \end{cases} \tag{4}$$

where notations $_{x=a}$ and $_{x=0}$, etc., indicate the faces which do not include points and vertices on the edge of the unit cell.

The edge of the unit cell belongs to two adjacent faces, and each point on the edge should meet two face displacement constraint equations, so boundary conditions of the edge should be re-derived. The number of all edges and vertices of the unit cell are shown in Fig.2. The twelve edges of the unit cell can be classified into three edges(IX,X,XI and XII) parallel to the x axis, edges(V,VI,VII and VIII) parallel to the y axis, and edges(I,II,III and IV) parallel to the z axis. It is obvious that each group of edges are independent, and any one edge from each group can be obtained by a certain translational symmetry transformation from any other edge in the same group. Edge I is selected for example. Edges II, III and IV can be transformed from edge I by translational symmetry transformations (i=1, j=0, k=0), (i=1, j=1, k=0) and (i=0, j=1, k=0), respectively. The other two groups of edges also have similar transformations. Thus, the temperature relationships between these edges are as follows:

Excerpt from ISBN 978-3-00-053387-7

$$\begin{cases} T_{\mathrm{II}} - T_{\mathrm{I}} = aT_x^0 \\ T_{\mathrm{III}} - T_{\mathrm{I}} = aT_x^0 + bT_y^0 \\ T_{\mathrm{IV}} - T_{\mathrm{I}} = bT_y^0 \end{cases} \tag{5}$$

$$\begin{cases} T_{\mathrm{VI}} - T_{\mathrm{V}} = aT_x^0 \\ T_{\mathrm{VII}} - T_{\mathrm{V}} = aT_x^0 + hT_z^0 \\ T_{\mathrm{VIII}} - T_{\mathrm{V}} = hT_z^0 \end{cases} \tag{6}$$

$$\begin{cases} T_{\mathrm{X}} - T_{\mathrm{IX}} = bT_y^0 \\ T_{\mathrm{XI}} - T_{\mathrm{IX}} = bT_y^0 + hT_y^0 \\ T_{\mathrm{XII}} - T_{\mathrm{IX}} = hT_z^0 \end{cases} \tag{7}$$

All vertices of the unit cell are include in Eq.(7), because each of them is shared by three intersecting edges belonging to three different equation, and any vertex can be transformed by another in a certain translational symmetry transformation. Thus, the relations of the vertices are as follows:

$$\begin{cases} T_2 - T_1 = aT_x^0 \\ T_3 - T_1 = aT_x^0 + bT_y^0 \\ T_4 - T_1 = bT_y^0 \\ T_5 - T_1 = hT_z^0 \\ T_6 - T_1 = aT_x^0 + hT_z^0 \\ T_7 - T_1 = aT_x^0 + bT_y^0 + hT_z^0 \\ T_8 - T_1 = bT_y^0 + hT_z^0 \end{cases} \tag{8}$$

2.2. Solution of equivalent parameters

The steady state thermal analysis equation is:

$$\lambda_x \frac{\partial^2 T}{\partial x^2} + \lambda_y \frac{\partial^2 T}{\partial y^2} + \lambda_z \frac{\partial^2 T}{\partial z^2} + \left(\lambda_{xy} + \lambda_{yx}\right)\frac{\partial^2 T}{\partial x \partial y} + \left(\lambda_{xz} + \lambda_{zx}\right)\frac{\partial^2 T}{\partial x \partial z} + \left(\lambda_{yz} + \lambda_{yx}\right)\frac{\partial^2 T}{\partial y \partial z} = 0 \tag{9}$$

where T is the temperature, $\lambda_x, \lambda_y, \lambda_z, \lambda_{xy}$ etc. are the non-isotropic thermal conductivities.

From Eq.(9) and boundary conditions, the temperature distribution can be calculated by numerical simulation. The heat flux components related to temperature gradients at x,y,z directions are shown as follows:

$$\begin{cases} q_x^0 = -\lambda_x^0 T_x^0 - \lambda_{xy}^0 T_y^0 - \lambda_{xz}^0 T_z^0 \\ q_y^0 = -\lambda_{yx}^0 T_x^0 - \lambda_y^0 T_y^0 - \lambda_{yz}^0 T_z^0 \\ q_z^0 = -\lambda_{zx}^0 T_x^0 - \lambda_{zy}^0 T_y^0 - \lambda_z^0 T_z^0 \end{cases} \tag{10}$$

where q_x^0 , q_y^0 , q_z^0 are the heat flux in x,y,z directions, respectively. T_x^0 , T_y^0 , T_z^0 are temperature

Excerpt from ISBN 978-3-00-053387-7

gradients that could be calculated by the post-processing of the numerical results. λ_x^0, λ_y^0, λ_z^0 are thermal conductivities to be determined.

After incorporating periodic boundary conditions in FE analyses, concentrated heat fluxes Q_x , Q_y or Q_z can be treated as key degrees of freedom to the model. After calculating by finite element analyses, corresponding temperature can be obtained. Heat fluxes are related to the concentrated heat fluxes as follows:

$$\begin{cases} Q_x = A_x q_x^0 \\ Q_y = A_y q_y^0 \\ Q_z = A_z q_z^0 \end{cases} \tag{11}$$

where A_x, A_y, A_z are the area of the unit cell which are perpendicular to the concentrated heat flux. The effective thermal conductivity of the composite represented by the unit cell concerned can be calculated as follows:

$$\begin{aligned} &\lambda_x^0 = q_x^0 / T_x^0 = Q_x / A_x T_x^0, \text{when } T_y^0 = T_z^0 = 0, \\ &\lambda_y^0 = q_y^0 / T_y^0 = Q_y / A_y T_y^0, \text{when } T_x^0 = T_z^0 = 0 \\ &\lambda_z^0 = q_z^0 / T_z^0 = Q_z / A_z T_z^0, \text{when } T_x^0 = T_y^0 = 0 \end{aligned} \tag{12}$$

When solving the thermal expansion, the stress-strain relationship of the material in the heating process is as follow:

$$\sigma_{ij} = C_{ijmn}\varepsilon_{mn} - C_{ijmn}\lambda_{mn}\Delta T \quad (i, j, m, n = x, y, z) \tag{13}$$

where C_{ijmn}, σ_{ij}, ε_{mn} and λ_{mn} are stiffness tensor, stress tensor, strain tensor and thermal expansion coefficient, respectively. ΔT is the temperature difference of the two parallel faces. First, when ΔT=0, incorporating 6 groups of independent strain load and periodic displacement boundary conditions, the corresponding stiffness matrix of the material can be calculated. Second, when $\Delta T \neq 0$, the unit cell is fixed to make sure that ε_{mn}=0, the thermal expansion coefficient could be calculated with the corresponding stiffness matrix calculated before.

3. Numerical model

3.1. Unit cell for yarn

The scale of undulations of yarns is much greater than that of fiber diameters and therefore yarns in a woven composite can be reasonably idealized as an UD fiber-reinforced composite. Assuming that fibers distribution in yarns is uniform and the fibers show a reasonably circular shape with a fairly uniform diameter. As an idealization, rectangle unit cells can be obtained from cross section of the yarn as shown in Fig.3.

Excerpt from ISBN 978-3-00-053387-7

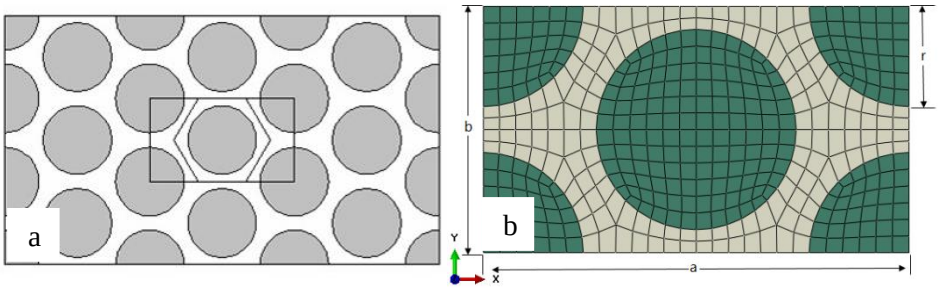

Figure 3. Unit cell for yarn: (a) fiber accumulation mode, (b) The FEM of unit cell

3.2. Unit cell for fine woven pierced c/c composite

In real application of composite materials, there are a significant number of layers of woven fabric stacked together to build up the desirable thickness. Then the materials are pierced by carbon fiber bundles in Z direction according to the warp and weft density as shown in Fig.4. For the pattern of plain weave, all layers can be reproduced by another by a simple translation. Therefore, the material is period in the x, y and z directions, the cuboid unit cell can be built up to present the composite as shown in Fig.5.

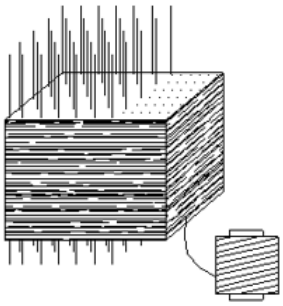

Figure 4. Schematic diagram of fine woven pierced fabric cell structure

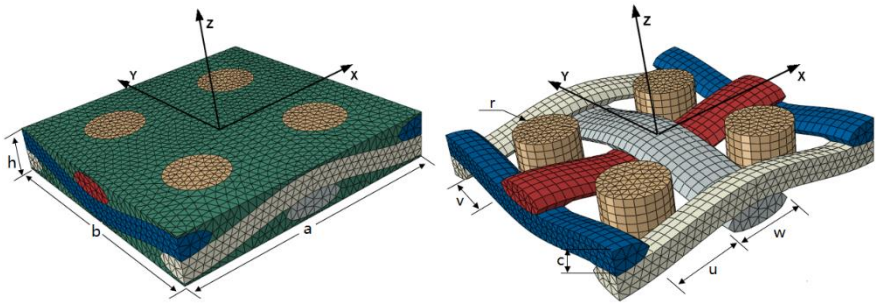

Figure 5. The unit cell for fine woven pierced c/c composite

In order to simplify the finite model, the cross section of Z-directional yarns are assumed circle, the cross section of warp and weft are ellipse. The bonding between yarns and matrix is assumed to be perfect and there are no void in the unit cell. The three dimensions of the unit cell obtained from scanning electron microscope (SEM) analyses are a=b=2.60mm，h=0.44mm. The axes of warp and weft are described as the Eq.(14). The cross section of warp and weft are w=0.61mm，c=0.20mm and

Excerpt from ISBN 978-3-00-053387-7

the spacing between two neighboring yarns is u=v=0.69mm. The radius of Z-directional yarn is r=0.29mm. The volume fraction of the yarns in the unit cell is 48.48%.

$$Z_x = \pm\frac{c}{2}\cos(\pi x/a)$$
$$Z_y = \pm\frac{c}{2}\cos(\pi y/b) \quad (14)$$

4. Analysis results and discussion

4.1. Material properties

The thermo-physical properties of fibers and matrix are shown in Tab.1. Another four models with different yarn volume fraction have been built up for further research as shown in Fig.6.

Table 1. Elastic and thermos-physical properties of T-300 and carbon matrix[10]

		Fiber (T300)	Matrix
Density (kg/m^3)		1760	1820
Specific heat (J(kg·K)$^{-1}$)		711	115.9
Thermal conductivity (W/(m·K))	Radial	10	70.36
	Axial	100	
Elastic modulus (Mpa)	E_{11}	210	5.1
	E_{22}	20.4	
	E_{33}	20.1	
Shear modulus (Mpa)	G_{12}	10	—
	G_{23}	20	
	G_{13}	10	
Poisson ratio	ν_{12}	0.16	0.3
	ν_{23}	0.3	
	ν_{13}	0.16	
Thermal expansion coefficient (10^{-6}/K)	Transverse	-0.7	5
	Longitudinal	8.85	

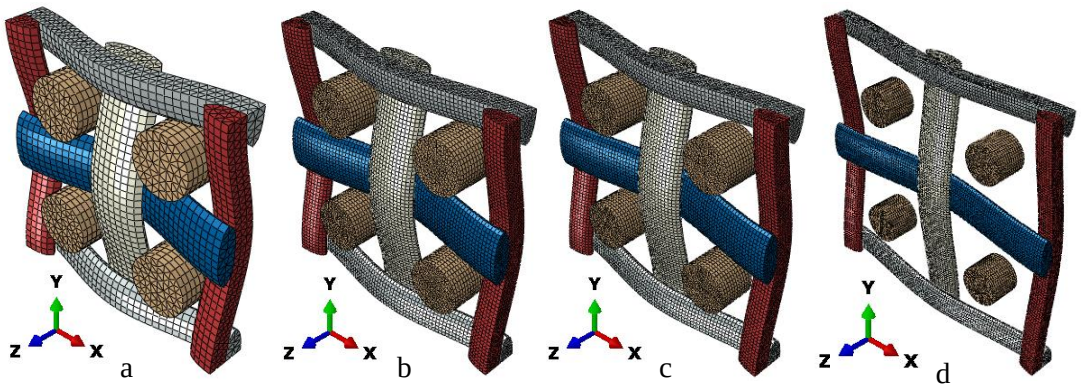

Figure 6. Fine woven pierced c/c composites with varies of yarn volume fraction: (a) 53.75% yarn volume fraction, (b) 44.35% yarn volume fraction, (c) 40.40% yarn volume fraction, (d) 27.98% yarn volume fraction

Excerpt from ISBN 978-3-00-053387-7

4.2. Thermal conductivity

The thermal conductivity of fine woven pierced c/c composites with varies of yarn volume fraction predicted from FEM is shown in Fig.7. With the increase of yarn volume fraction, both transverse and longitudinal thermal conductivities decreased. It can been seen from Tab.1 that, although the matrix thermal conductivity is lower than fiber axial thermal conductivity, it is much higher than fiber radial thermal conductivity. The thermal conductivity of composite is consistent with the rule of mixture partially, when the fraction of matrix with higher thermal conductivity gets lower, the overall thermal conductivity of the composite will decrease reasonably. The heat fluxes conducted in the composite are mainly along the axial direction of the yarns and the transverse direction of the fiber bundle has a blocking effect on the conducting. As the volume fraction of Z-directional yarns is much lower than XY-directional interlaced yarns, the longitudinal thermal conductivity is lower than the transverse thermal conductivity in the composite. Fig.7 also shows with the increase of the yarn volume fraction the gap between longitudinal thermal conductivity and transverse thermal conductivity was gradually reduced. This provides a practical method for the design of materials, which can be realized by adjusting the density of warps and wefts, when the material needs to have different thermal conductivity ratios in the two directions.

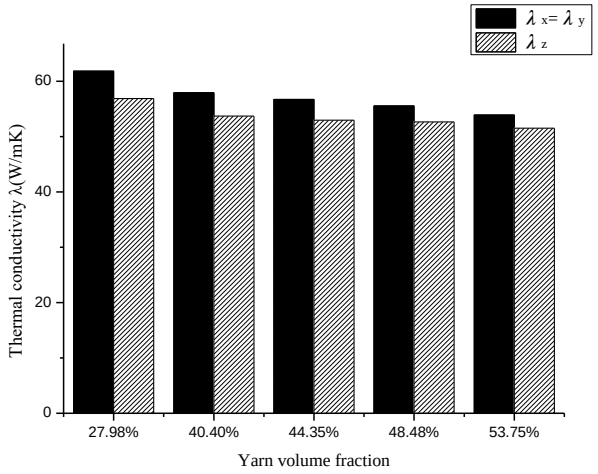

Figure 7. Effective thermal conductivities of the fine woven pierced c/c composites with varies of yarn volume fraction predicted from FEM

The heat flux distributions in composite at a yarn volume fraction of 48.48%, loaded with concentrated heat flux Q_x=1KW , are shown in Fig.8. It can be seen that high values heat fluxes are mostly found in warp yarns, indicating that warp yarns are mainly bearing heat in this loading case. The heat flux concentrations are mainly located at the intersection of yarns and in the surrounding matrix. The maximum values of the heat flux is 1739W/m^2 in the yarns and 1459W/m^2 in the matrix, respectively.

Excerpt from ISBN 978-3-00-053387-7

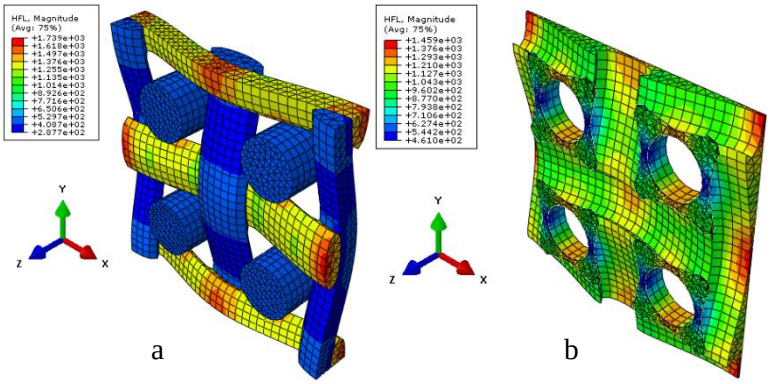

Figure 8. Heat flux distributions in fine woven pierced c/c composite under Q_x=1KW : (a) yarns, (b) sectioned view of matrix

4.3. Thermal expansion coefficient

The thermal expansion coefficient of fine woven pierced c/c composites with varies of yarn volume fraction predicted from FEM is shown in Fig.9. It can be seen that no matter what the yarn volume fraction is, the thermal expansion coefficient of the composite is nearly unchanged. The difference between longitudinal thermal expansion coefficient and transverse thermal expansion coefficient is very small too. In contrast to the other thermo-physical properties of composite, the thermal expansion coefficient is related to the elastic properties of the material. A significant constraints will be effected on the interface when the elastic properties of components differ greatly. Thus, even if the fraction volume varies greatly, the overall thermal expansion coefficient may remain stable.

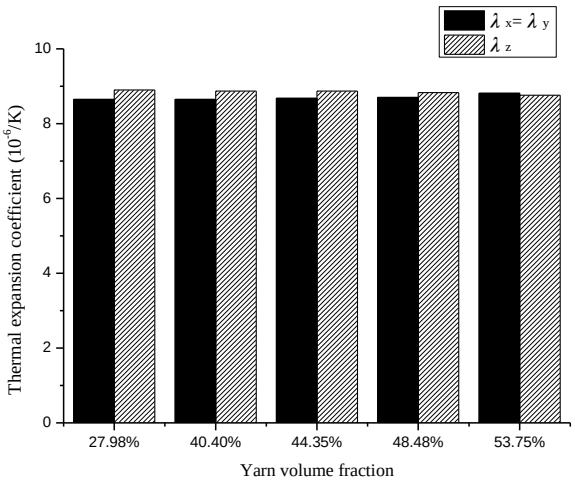

Figure8. Thermal expansion coefficients of the fine woven pierced c/c composites with varies of yarn volume fraction predicted from FEM

5. Conclusions

This work build up a series of models to predict the thermo-physical properties of the fine woven pierced c/c composites which can be a reference for the industrial designers when they study and

Excerpt from ISBN 978-3-00-053387-7

optimize composite materials varying the factors that affect their thermo-physical properties. From the numerical results following conclusion can be made.

(1) Increasing yarn volume fraction decreases transverse and longitudinal thermal conductivities both. And the gap between longitudinal thermal conductivity and transverse thermal conductivity was reduced gradually.

(2) The yarns are mainly bearing heat. The heat flux concentrations are mainly located at the intersection of yarns and in the surrounding matrix.

(3) No matter what the yarn volume fraction is, the thermal expansion coefficient of the composite is nearly unchanged.

References

[1] Shi Z H, Li K Z, Li H J, and Tian Z. Research status and application advance of heat resistant materials for space vehicles. *Materials Review,* 2007,08:15-18.
[2] Grujicic M, Zhao CL, Dusel EC, Morgan DR, Miller RS, Beasley DE.Computational analysis of the thermal conductivity of the carbon–carbon composite materials. *Mater Sci* 2006;41(24):8244–56.
[3] Huang HS, Ganguli S, Roy AK. Prediction of the transverse thermal conductivity of pitch-based carbon fibers. *Compos Mater,* 2013.
[4] Zou M Q, Yu B M, Zhang D M, et al. Study on optimization of transverse thermal conductivities of unidirectional composites. *Journal of Heat Transfer,*2003,125(2):980-987.
[5] Woo K, Goo N S. Thermal conductivity of carbon-phenolic 8-harness satin weave composites. *Composite Structures,*2004,66(1-4):521-526.
[6] D. Bigaud, J.M. Goyheneche, and P. Hamelin. A global-local nonlinear modelling of effective thermal conductivity tensor of textile-reinforced composites. *Composites Part A* 32, 1443 (2001).
[7] J.K. Farooqi and M.A. Sheikh. Finite element modelling of thermal transport in ceramic-matrix composites. *Comput. Mater. Sci.* 37, 361 (2006).
[8] J. Schuster, D. Heider, K. Sharp, and M. Glowania. Thermal conductivities of three-dimensionally woven fabric composites. *Compos. Sci. Technol.* 65, 2085 (2008).
[9] Li H Z, Li S G, Wang Y C, Prediction of effective thermal conductivities of woven fabric composites using unit cells at multiple length scales. *Journal of Materials Research,* 2011, 26(03):384-394.
[10] Zhang M, Investigation on the thermophysical properties of multi-directional textile composites,2008.

Excerpt from ISBN 978-3-00-053387-7